

Supporting Information

Hierarchical hollow metal nanostructure arrays for selective CO₂ conversion

Authors

James W. Maina^{1*}, Jennifer M. Pringle¹, Joselito M. Razal¹, Stella Aslanoglou^{2,3,4}, Roey Elnathan^{2,3}, Nicolas H. Voelcker^{2,3}, Ludovic F. Dumée^{5,6*}

Affiliations

1 Deakin University, Geelong, Institute for Frontier Materials, Waurn Ponds, 3216, Victoria, Australia

2 Melbourne Centre for Nanofabrication Victorian Node of the Australian National Fabrication Facility 151 Wellington Road, Clayton, VIC 3168, Australia

3 Monash Institute of Pharmaceutical Sciences, Monash University, 381 Royal Parade, Parkville, Victoria, 3052, Australia.

4 School of Physics, The University of Melbourne, Melbourne, Victoria 3010, Australia

5 Khalifa University, Department of Chemical Engineering, Abu Dhabi, United Arab Emirates

6 Research and Innovation Center on CO₂ and Hydrogen (RICH), Khalifa University, Abu Dhabi, United Arab Emirates

Experimental

Convective assembly deposition of polystyrene beads.

Polystyrene (PS) bead monolayer was deposited on silicon wafer using the convective assembly technique, as previously reported.¹ The experimental setup includes a compact sub-hertz pendulum vibration isolation system (TMC), a 50 mm motorized translation stage (MTS50-Z8, Thorlab, Inc.), and a microscope glass slide that is used as a blade for PS bead deposition. The slide was adjusted to leave a small space between the bottom edge of the slide and the silicon substrate. 15 μl of polystyrene suspension (3 μm , 2.5 % w/v) was carefully injected at the space between the blade and the silicon substrate (3 x 3.5 cm) forming a meniscus, after which the movement of the blade over the substrate was initiated. The speed of blade was controlled to optimize the homogeneity of the PS monolayer.

Deep reactive ion etching (DRIE)

Prior to deep reactive ion etching, the PS monolayer was subjected to oxygen plasma reactive ion etching,¹ to shrink the size of the PS beads. The reduced size PS beads served as a mask for the subsequent silicon etching. Both the oxygen plasma etching and silicon etching were carried out in a Plasmalab100 ICP380 deep reactive ion etcher (Oxford Instruments). The oxygen plasma etching was carried out for 30 s using an oxygen flow rate of 100 sccm, an inductively coupled plasma (ICP) power of 100 W and a bias power of 50 W.

Silicon etching was performed by alternate cycles of passivation and etching steps (Bosch process). During the etching step a flow rate of 150 sccm SF_6 and 3 sccm C_4F_8 was used with ICP power of 2000 W and bias power of 20 W.¹ During the passivation step a flow rate of 150 sccm C_4F_8 and 3 sccm SF_6 was used with ICP power of 1500 W and bias power of 5 W. This resulted in an array of vertically aligned cylindrical pillars.

The PS beads were then removed via sonication in the presence of ethanol, and the substrate was further subjected to a Pseudo-Bosch etching process to convert the cylindrical pillars into cone-shaped nanostructures. The Pseudo-Bosch process involved simultaneously exposing the cylindrical pillars to both SF₆ and C₄F₈ at flow rates of 100 and 40 sccm respectively, with ICP power of 1500 W and bias power of 50 W. The etching was carried out for a duration of 195 seconds.

Preparation of PVA templates

The nanostructured silicon substrate was placed on a TEFLON mould with the cone-shaped nano patterns facing upwards. The mould was then filled with 5 mL of polyvinyl alcohol (PVA) release agent, making sure the substrate was completely submerged, and then dried at room temperature for 24 h, to allow the PVA film to cure. Upon drying the PVA film was carefully peeled off and used as a template for metal deposition.

Metal deposition by magnetron sputtering.

Magnetron sputtering was carried out using Anatech Hummer BC 20 RF/DC system, with PVA template as the substrate. The template was placed so as to expose the wider openings of the micro-moulds to the sputtering target. Prior to deposition, the chamber was evacuated to 10⁻⁶ Torr, after which Ar was introduced into the chamber at a flow rate of 30 sccm. Copper deposition was carried out in two stages, first deposited at 100 W DC for 45 min, and then at 300 W for 1 h. Silver was deposited at 150 W DC for 1 h, while Ni and Pd were deposited at 300 W DC for 1h and 20 min respectively.

Electrochemical tests

Cyclic voltammetry (CV) and electrocatalytic tests were carried out using a H-cell electrochemical reactor, with Ag/AgCl reference electrode, Pt as counter electrode and the hollow nanostructured copper (0.5 x 1 cm) or plain copper film as the working electrode. The thin copper films were mounted on a carbon cloth (1071 HCB carbon cloth), using graphite/epoxy composite glue to facilitate handling. Cyclic voltammetry was carried out at a scanning rate of 50 mV/s between 0.4 to -2.7 V, while the electrocatalytic tests were carried out at applied potential of between -1.8 to -2.4 V. The counter electrode cell was filled with 15 mL of aqueous solution of potassium bicarbonate (0.5M), while the working electrode was filled with 15 mL of 1-ethyl-3-methylimidazolium acetate [C2mim][OAc] (150 mM) in dimethyl acetamide solvent. The electrolyte in the working compartment was saturated with CO₂ by purging for 30 min prior to the electrocatalytic reactions. Gaseous products were analysed using MultiRae detector, equipped with CO, H₂ and CH₄ electrochemical sensors, as well as with Gas chromatograph (GC, Trace 1310) equipped with thermal conductivity detector (TCD) and TG – BOND Q column. Final concentrations for the gases were computed from calibration curves (**Figure S7**), generated using a standard gas with known concentrations (Supplied by Air Liquide). CO and H₂ were calculated from the equations $y = 0.04697x + 0.38333$ and $y = 0.3031x + 0.857$ respectively, where x is the value obtained from the sensor while y is the actual amount of the gas in moles. The electrolyte solution was also collected and analysed using GC equipped with flame ionization detector (FID) and Porabond u column, and with nuclear magnetic resonance spectroscopy (NMR) to check for any liquid products.

Measurement of electrochemical surface area

Electrochemical surface area (ECSA) was measured by double layer capacitance method, as reported in the literature.^{2, 3} At first, a series cyclic voltammetry (**Figure 4a and b**) were carried out at non-faradaic region (0 - 100 mV) at various scan speed of between 10 mV/s to 100 mV/s. Current density corresponding to 50 mV was then plotted against the scanning rate, to produce a straight line (**Figure 4c and d.**), whose slope correspond to double layer capacitance(C_{DL}) of the material.² The ECSA was then calculated from the ratio of the cdl and the specific capacitance of Cu, which 0.02 mF cm^{-2} .⁴

Supplementary Figures

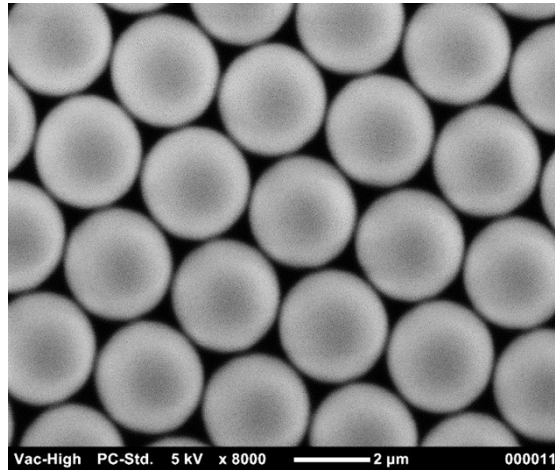


Figure S1. SEM image of polystyrene bead monolayer on the surface of silicon wafer.

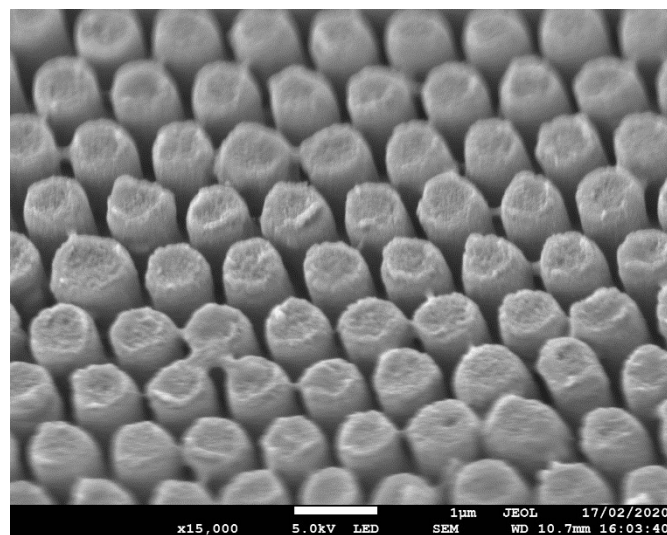


Figure S2. Cu nanorods obtained from magnetron sputtering on a PVA template having micro-moulds with depth of 1 μm and diameter of 500 nm.

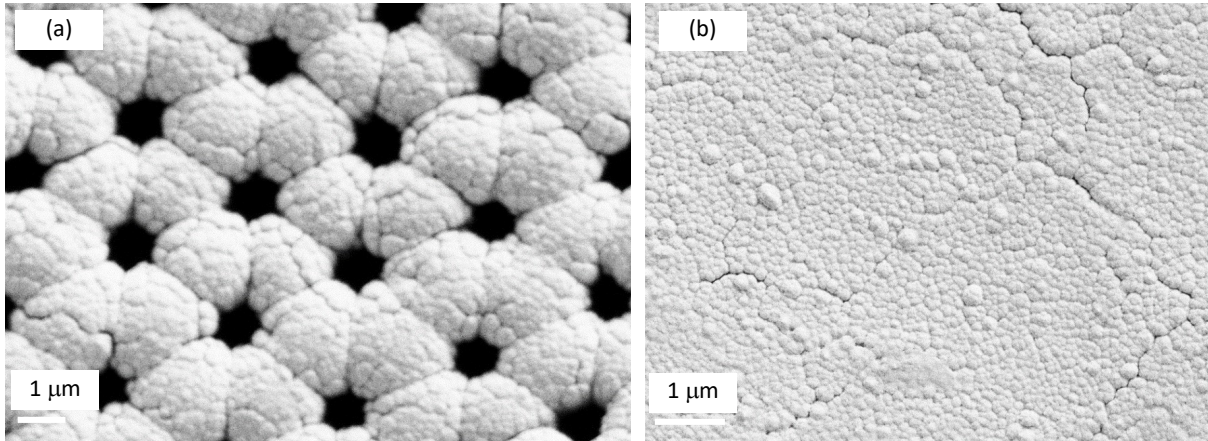


Figure S3. (a) Surface morphology of the PVA template after partial deposition of Cu, (b) surface morphology of the PVA template completely covered by the Cu film.

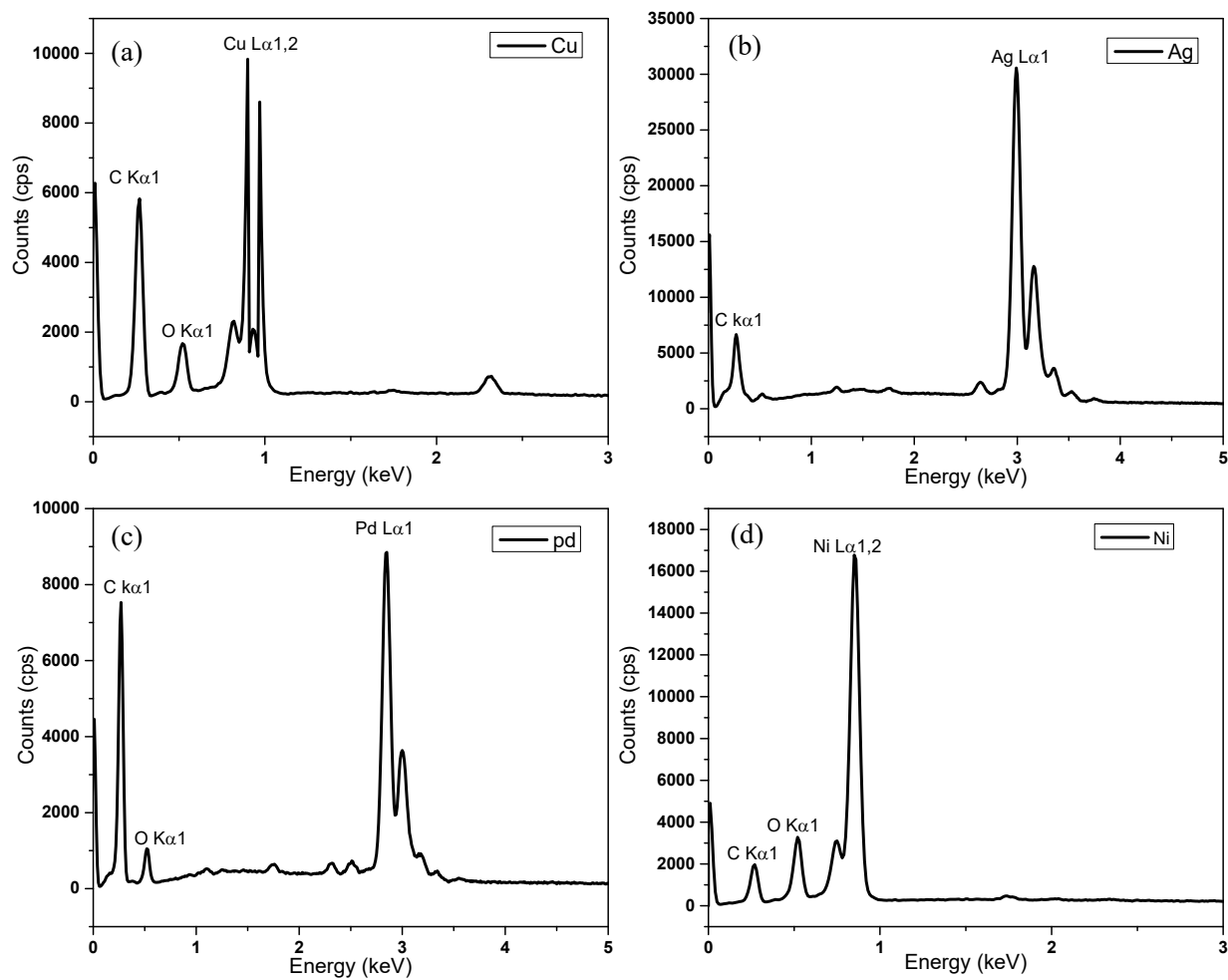


Figure S4. EDX analysis for (a) Cu, (b) Ag, (c) Pd and (d) Ni hollow nanostructures.

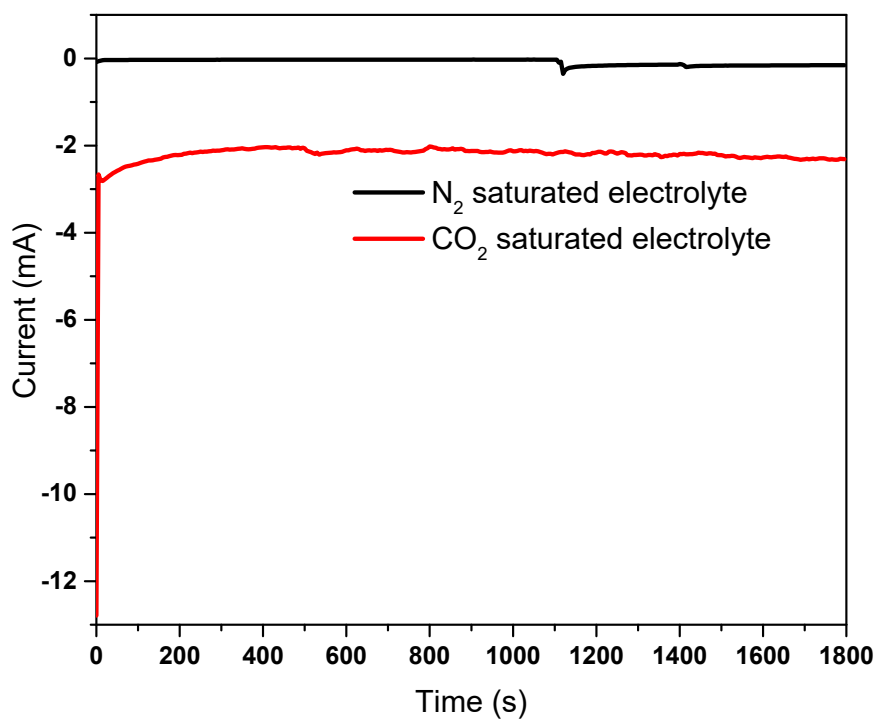


Figure S5. Comparison of the current density for electrocatalytic conversion in N₂ saturated electrolyte and CO₂ saturated electrolyte at an applied potential of -2.2V. The current density remained close to zero in N₂ saturated electrolyte indicating there was no catalytic reactions in the absence of CO₂.

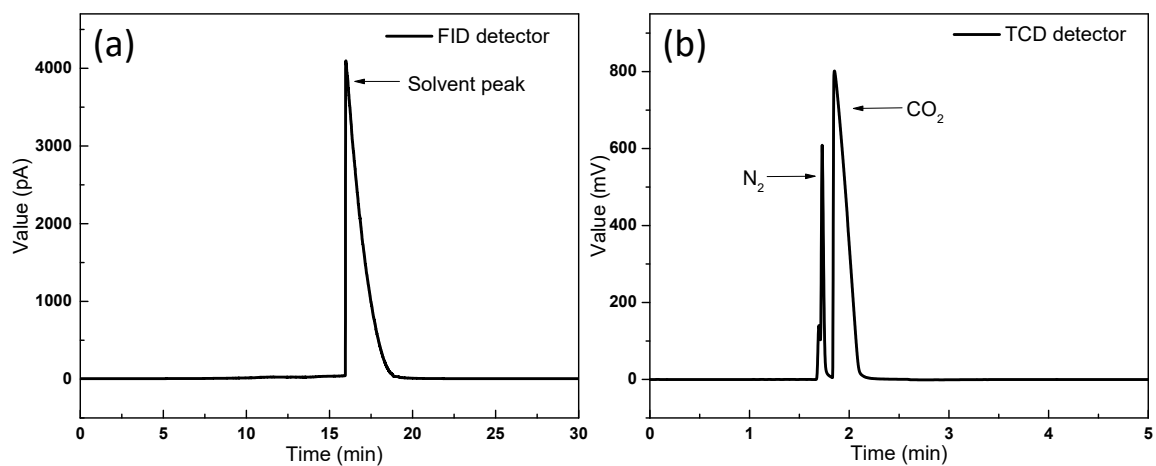


Figure S6. Gas chromatograph spectrum for the analysis of (a) Liquid products using FID detector, (b) Gaseous product using TCD detector.

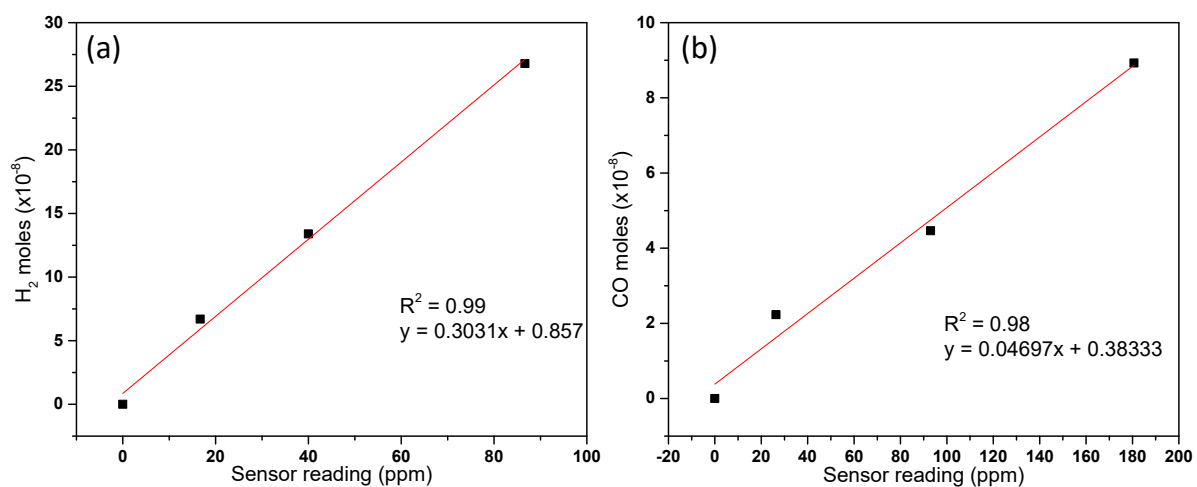


Figure S7. Calibration curves for the quantification of H₂ and CO gases.

References

1. Chen, Y.; Aslanoglou, S.; Gervinskas, G.; Abdelmaksoud, H.; Voelcker, N. H.; Elnathan, R., Cellular Deformations Induced by Conical Silicon Nanowire Arrays Facilitate Gene Delivery. *Small* **2019**, *15* (47), 1904819.
2. Babar, N.-U.-A.; Joya, K. S., Spray-Coated Thin-Film Ni-Oxide Nanoflakes as Single Electrocatalysts for Oxygen Evolution and Hydrogen Generation from Water Splitting. *ACS Omega* **2020**, *5* (19), 10641-10650.
3. Wang, J.; Bao, Y.; Cui, C.; Zhang, Z.; Li, S.; Pan, J.; Zhang, Y.; Tu, G.; Wang, J.; Li, Z., Fabrication of dispersive α -Co(OH)₂ nanosheets on graphene nanoribbons for boosting their oxygen evolution performance. *Journal of Materials Science* **2019**, *54* (10), 7692-7701.
4. Zhu, P.; Zhao, Y., Effects of electrochemical reaction and surface morphology on electroactive surface area of porous copper manufactured by Lost Carbonate Sintering. *RSC Advances* **2017**, *7* (42), 26392-26400.